Hindawi Publishing Corporation
Advances in Mechanical Engineering
Volume 2013, Article ID 874673, 6 pages
http://dx.doi.org/10.1155/2013/874673

Research Article

Stress Analysis in Fruits

L. Fenyvesi,[1] D. Fenyvesi,[2] and A. Csatár[1]

[1] *Hungarian Institute of Agricultural Engineering, Tessedik Sámuel Street 4, Gödöllő 2100, Hungary*
[2] *Donát Bánki Faculty of Mechanical and Safety Engineering, Óbuda University, Népszínház Street 8, Budapest 1081, Hungary*

Correspondence should be addressed to L. Fenyvesi; fenyvesi.laszlo@gmgi.hu

Received 29 August 2013; Revised 10 November 2013; Accepted 19 November 2013

Academic Editor: Magd Abdel Wahab

It is a known phenomenon that loads during fruit treatment (e.g., harvesting, transport, and manipulating) result in the damage of product parts, primarily below the surface. The maximum stress likely develops inside the fruit, which leads to its damage. This phenomenon was analysed in a general manner (general material properties, unit load) by finite element method (FEM) simulations on an apple and a pear. The shell was found to have a significant effect on the developed stress state, especially for juicy fruits. The mechanism that determines how the stress properties of tomatoes affect the stress state was analysed. According to our model, the stress maxima develop in the middle of the analysed fruits. Such stress maxima might be the reason for the inner damage, which, in the case of a missing healing period, results in fruit breakage.

1. Introduction

There is a connection between the mechanical damage of a fruit and the stress state developed while loading the fruit [1]. Any damage and injury on the fruit surface is easy to identify [2]. The occurrence of damage below the shell has already been proven by several researchers. This phenomenon has been observed by Holt et al. [3] for apples and pears. Similar phenomena have been detailed by O'Brian et al. [4] for peaches and by Fridley and Adrian [5] for pears.

The discoloration of potatoes near to the surface has been analysed by Birth [6] using X-ray equipment, and he has indicated that the damage was caused by the load.

Frederich [7] provided the first strong explanation for the above phenomenon. Puchalski and Brusewitz [8] found that, in some cases, it is possible that the resulting stress maximum does not develop on the surface and that fruit is more resistant against shear stress.

The material inhomogeneity of the fruit essentially affects the resulting stress state. Four separated parts of the fruit can be observed: shell, flesh, core, and seed [9]. The different parts of the fruit affect the resulting stress state differently; for example, the effect of the shell is more important in tomatoes than in apples [10]. The complex structure of fruits requires the use of numerical modelling for its mechanical analysis [11]. The finite element method (FEM) is generally used to analyse complex mechanical interactions [12, 13], as well as to analyse the effect of the fruit parts [14, 15]. The discrete element method (DEM) was recently used to analyse the storage and transport of fruit batches [16, 17].

The skin is usually considered as a fruit part with different properties [18]; however, this solution does not consider the skin straightness or its fruit covering effect. There are some solutions available for the modelling of the contract stress state developing inside a sphere with known features and known skin covering properties [19]. The determining of the strength effect of the skin has been already shown by micromechanical modelling of the yeast cell wall [20].

There was no literature found either on the analysis of the stress state within the fruit or on the effect of the fruit shell.

Our aim was to determine the resulting stress state of fruits (apples and pears) for a given load as well as the role of the potato shell.

2. Materials and Methods

2.1. Mechanical Modelling of Fruits. Fruit injuries are generally caused by short time mechanical loads or impacts. The load on the fruit surface deforms the product. The mechanical

state can be determined by the displacement, the deformation field, and the resulting strain field. Usually, the maximum of a strength field is the point that exceeds the so-called biological yield point, beyond which the cell structure will be destroyed and finally result in the decomposition of the product.

The complex form and the complicated structure make the analytical calculation of the mechanical stress field impossible. In this case, the finite element method provides the most useful and the most convenient solution under the available options.

Fruit models must be prepared for the calculations, which will be considered as rotationally symmetric bodies. The symmetry axis of the model presented in a cut along the half meridian coincides with the y-axis.

The fruit consists of four separated parts: shell, flesh, core and seed.

In the calculations, the applied FEM element types were the following:

TRIANG3: two-dimensional three-node solid element, axial-symmetric—with analysis option (flesh, core, and seed),

SHELLAX: axial-symmetric two-node, conic shell element (fruit shell).

Material properties must be defined during the static calculations for each element type.

The buildup of the fruit load is assumed to be rapid; therefore, the relationship between the load and the deformation can be defined as an approximately linear elastic material model. However, the rheological equations provide a more accurate solution for the behaviour of vegetable materials. Isotropic behaviour of the material has been assumed because of the high moisture content.

The stress-elongation function of any axial symmetric model with elastic material properties is isotropic:

$$\begin{bmatrix} \sigma_r \\ \sigma_\Theta \\ \tau_r \\ \tau_\Theta \end{bmatrix} = \frac{E(1-\nu)}{(1+\nu)(1-2\nu)} \times \begin{bmatrix} 1 & \frac{\nu}{1-\nu} & 0 & \frac{\nu}{1-\nu} \\ \frac{\nu}{1-\nu} & 1 & 0 & \frac{\nu}{1-\nu} \\ 0 & 0 & \frac{1-2\nu}{2(1-\nu)} & 0 \\ \frac{\nu}{1-\nu} & \frac{\nu}{1-\nu} & 0 & 1 \end{bmatrix} \times \begin{bmatrix} \varepsilon_r \\ \varepsilon_\Theta \\ \gamma_{r\Theta} \\ \varepsilon_z \end{bmatrix}. \quad (1)$$

The 4×4 flexibility material matrix can be seen to use 2 pieces of data: $E = E_X$ and $\nu = \mathrm{NU}_{XY}$.

The material properties used in our models are only the mean values of the literature parameters [21–23]; therefore, these are not characteristic for a single unit or species.

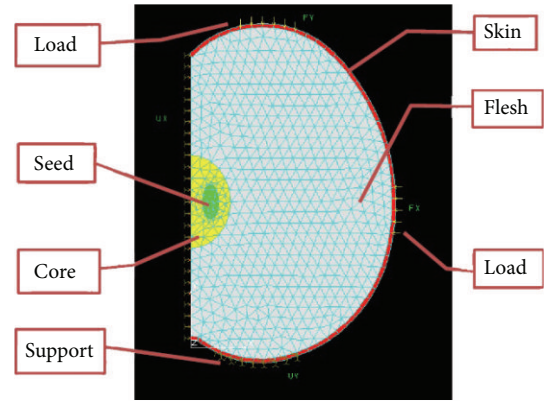

Figure 1: The buildup of the model "apple."

Table 1: Material properties of model apple.

Flesh	E_X	600 MPa
	NU_{XY}	0.3
Core	E_X	1000 MPa
	NU_{XY}	0.3
Seed	E_X	3000 MPa
	NU_{XY}	0.3
Skin	E_X	800 MPa
	NU_{XY}	0.3

E_X: Young's modulus, NU_{XY}: Poisson factor.

In addition, the exact values of the boundary conditions are not important because only the stress state distribution has been analysed. Therefore, a unit load was only applied at the given points in the models.

The load set of the fruit was a distributed load on the top and sideward; furthermore, a sustainment was used on the bottom and in the rotating axis to provide a balance.

2.1.1. The Finite Element Model of an Apple Can Be Seen in Figure 1. The set material properties are in Table 1.

2.1.2. The Finite Element Model of a Pear Can Be Seen in Figure 2. The applied FEM element types were as follows:

TRIANG: axial-symmetric three-node solid element (flesh, core),

SHELLAX: axial-symmetric two-node, conic shell element (fruit skin).

The load set of the fruit was a distributed load sideways; also, a sustainment was used on the bottom and in the rotating axis to provide a balance.

The set material properties are in Table 2.

2.2. Modelling the Mechanical Effect of the Shell. The potato was considered as an approximately rotationally symmetric body. The symmetry axis of the model presented in a cut along the half meridian coincides with the y-axis. The fruit consists of three separated parts: shell, flesh, and juice. The

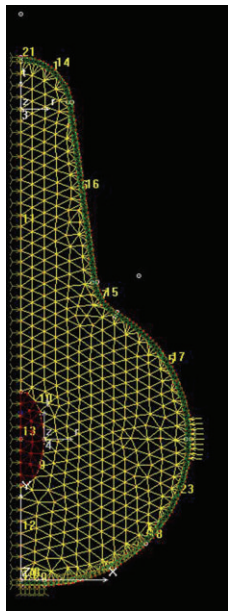

Figure 2: The finite element model of the "pear."

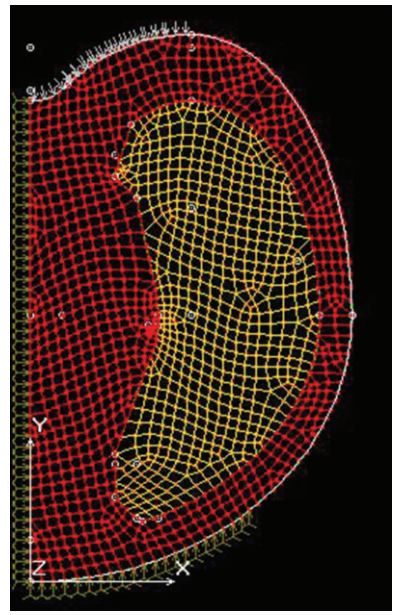

Figure 3: Modelling of the strength effect of the shell.

Table 2: The material properties of the pear model.

Flesh	E_X	400 MPa
	NU_{XY}	0.3
Core	E_X	1000 MPa
	NU_{XY}	0.3
Skin	E_X	800 MPa
	NU_{XY}	0.3

E_X: Young's modulus, NU_{XY}: Poisson factor.

Table 3: Material properties of the "shell model".

Juice	E_X	1000 MPa
	NU_{XY}	0.3
	G_{xy}	2 MPa
Flesh	E_X	500 MPa
	NU_{XY}	0.3
Shell	E_X	Variable (500–1000) MPa
	NU_{XY}	0.3

E_X: Young's modulus, NU_{XY}: Poisson factor, and G_{xy}: shear modulus.

first two items are solid, while the third one is liquid. The load set of the body was a distributed load on the top, with a sustainment used on the bottom and in the rotating axis to provide a balance (Figure 3).

The applied FEM element types were as follows:

(1) juice: PLANE2D, axial-symmetric, four-node element with liquid option,

(2) flesh: PLANE2D, axial-symmetric, four-node element with solid option,

(3) shell: SHELLAX, axial-symmetric, shell element (in a 0.2 mm thickness).

Table 3 lists the set material properties of shell.

The goal of our analysis is to determine the value and the location (coordinates) of the reduced σ stress maximum (belonging to the applied load). The effect of the shell rigidity on the maximal stress value by unchanged load was also analysed.

The shell (or membrane) stiffness in the technical calculations is determined by the following equation:

$$D = \frac{h^3}{12\left(1-\nu^2\right)}E = \frac{\left(2\cdot 10^{-1}\right)^3}{12\left(1-0.3^2\right)}E = 7.326\cdot 10^{-4}\cdot E\,\text{Nmm}, \quad (2)$$

where h is the shell (or plate) thickness, ν is the *Poisson factor*, and E is *Young's modulus*.

Different stiffness values were set by varying Young's modulus (because of computational reasons, this was the only parameter varied), and the inner stress calculations were performed by using this stiffness value. The shell stiffness as well as corresponding Young's modulus in brackets was used in some calculations. The zoomed picture below shows the nodes (ND) belonging to the tables containing the results (Figure 4 and Table 4).

3. Results and Discussion

Figure 5 shows the reduced σ stress distribution and its distortion during loading of an apple.

Note that the maximum reduced stress develops around the core. Figure 6 shows the reduced σ stress distribution during the loading of a pear.

The pictures of the stress distributions of an apple and a pear show that the maximal stress does not develop close to the shell.

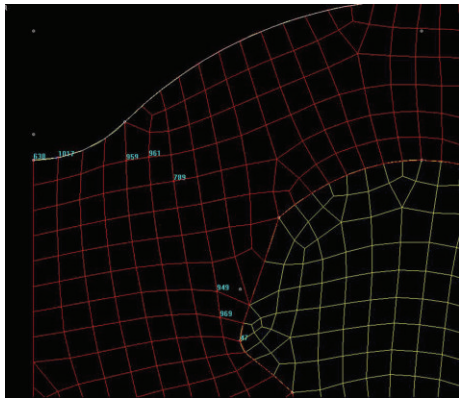

Figure 4: A zoomed picture of the nodes for the stress analysis ($D(0.5e3) = 0.3663$ Nmm).

Table 4: Location and value of the maximal stress points.

Skin stiffness (Nmm)	Maximal stress (MPa)	Location of the maximal stress (node)
0.7326	1.08	1017
1.465	0.99	1017
2.1978	0.85	47
2.93	0.797	47
3.663	0.7788	47
7.326	0.713	959

The pictures of the calculation results of the shell effect in the case of a potato show that the shell stiffness affects the size and place of the resulting stress (Figure 7).

Figure 4 shows the developed stress maximum points, and Table 4 lists its values.

The summarising pictures (Figure 7) show the connection between the stress and the stiffness. The plate stiffness is affected by the thickness (to the third power) and Young's modulus of the shell (the Poisson factor can be assumed to be constant). The picture proves the reasonable fact that the thicker and harder shell provides more protection against damage, although its measure cannot be estimated without extended calculations.

In addition, the largest stress was found to progress not on the surface but deeper. Moreover, according to Table 4, the maximal stress location was found to move away. The more rigid skin results in a maximal stress shifting from the skin towards the inside of the product.

Figure 8 shows the maximal stress developed in tomatoes for the same load along the shell stiffness. The more rigid shell was found to result in a lower maximal stress value within the product.

4. Conclusions

The results of the FEM modelling confirm that the stress state in fruits can be analysed universally (the mean value of the material properties and that of the defined biological load). The maximal reduced stress was found to develop

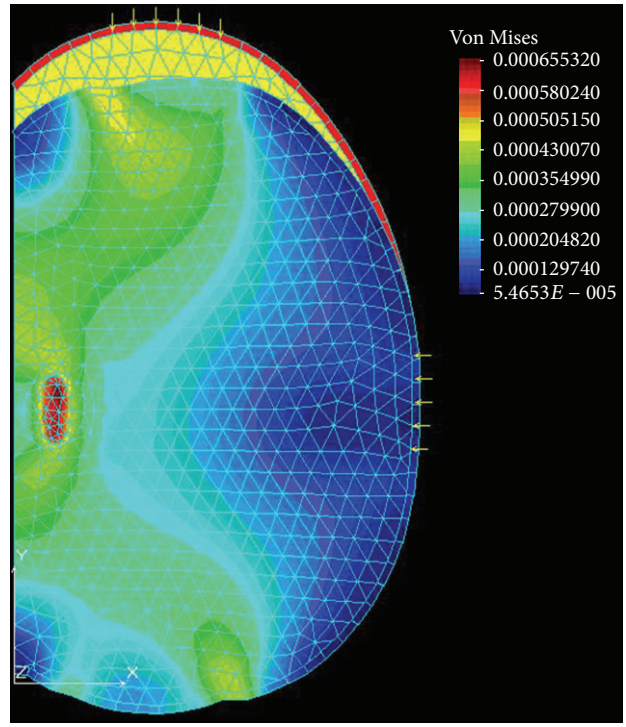

Figure 5: Numeric estimation for the stress distribution in an apple.

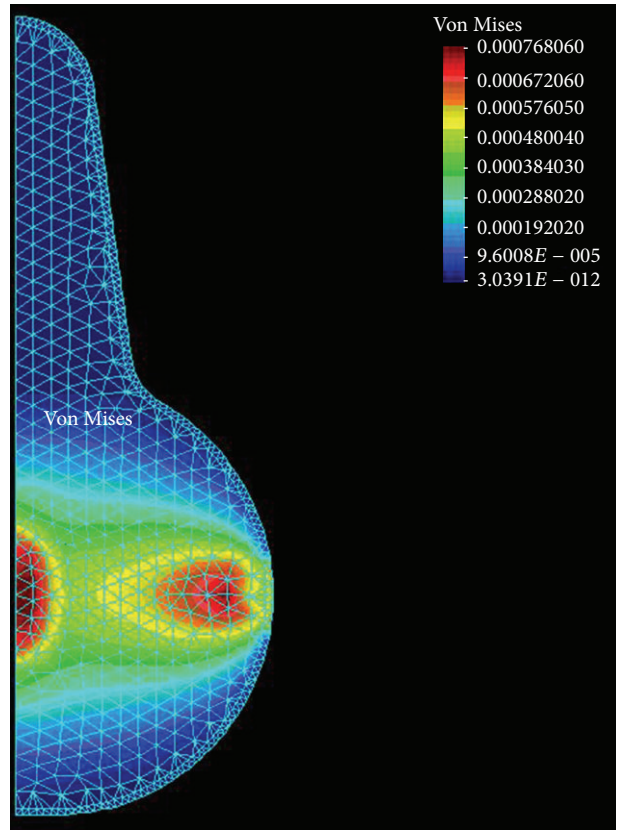

Figure 6: Stress distribution in a pear.

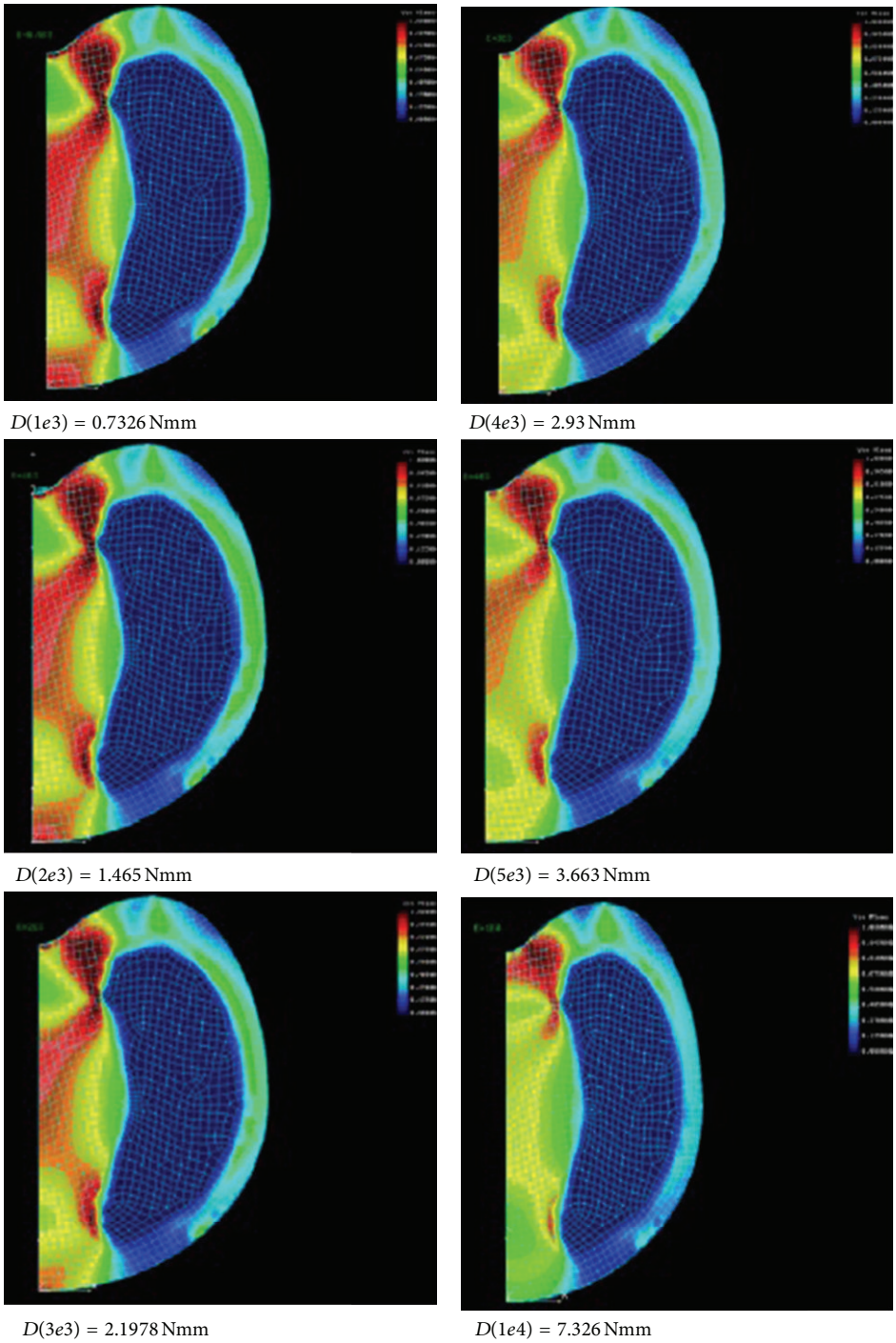

Figure 7: Some results of the stress analysis at different skin stiffness values.

near the core of an apple. This stress near the core was also found in the results of the pear. These simulation results indicate that the core operates as a stress accumulator part, which extraordinarily indicates that damage often occurs in the region near the core. The calculated results for a pear with the largest flesh thickness indicate that a local stress maximum develops below the surface. The shell of tomatoes plays an important role in the resulting stress distribution. A high shell rigidity was found to lower the inner stress maximum. This reduction is higher at the beginning, and its importance will be lower later on. Hence, a threshold value for the shell stiffness can be assumed, which should not be exceeded by plant selection because it will not result in a significant improvement of

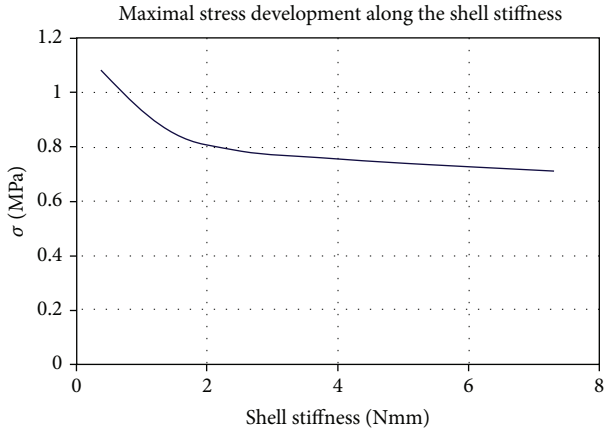

Figure 8: Relation between the shell stiffness and the maximal stress by a given load.

the mechanical resistance, but it already affects the culinary quality.

References

[1] S. J. Flood, T. F. Burks, and A. A. Teixeira, "Physical properties of oranges in response to applied gripping forces for robotic harvesting," *Transactions of the ASABE*, vol. 49, no. 2, pp. 341–346, 2006.

[2] N. Mohsenin, *Physical Properties of Plant and Animal Materials*, Pennsylvania State University, State College, Pa, USA, 1968.

[3] J. E. Holt, D. Schoorl, and C. Lucas, "Prediction of bruising in impacted multilayered apple packs," *Transactions of the ASABE*, vol. 24, no. 1, pp. 242–247, 1981.

[4] M. O'Brien, R. B. Fridley, J. R. Goss, and J. F. Schubert, "Telemetry for investigating forces on fruits during handling," *Transactions of the ASABE*, vol. 16, no. 2, pp. 245–247, 1973.

[5] R. B. Fridley and P. A. Adrian, "Mechanical properties of peaches, pears, apricots, and apples," *Transactions of the ASABE*, vol. 9, no. 1, pp. 135–138, 1966.

[6] G. S. Birth, "A nondestructive technique for detecting internal discolorations in potatoes," *American Potato Journal*, vol. 37, no. 2, pp. 53–60, 1960.

[7] R. Frederich, *Rheology Theory and Applications*, Academic Press, New York, NY, USA, 1966.

[8] C. Puchalski and G. H. Brusewitz, "Watermelon abrasion resistance parameters from friction tests," *Transactions of the ASAE*, vol. 39, no. 5, pp. 1765–1771, 1996.

[9] L.-X. Lu and Z.-W. Wang, "Dropping bruise fragility and bruise boundary of apple fruit," *Transactions of the ASABE*, vol. 50, no. 4, pp. 1323–1329, 2007.

[10] M. C. Alamar, E. Vanstreels, M. L. Oey, E. Moltó, and B. M. Nicolaï, "Micromechanical behaviour of apple tissue in tensile and compression tests: storage conditions and cultivar effect," *Journal of Food Engineering*, vol. 86, no. 3, pp. 324–333, 2008.

[11] T. R. Rumsey and R. B. Fridley, "Analysis of viscoelastic contact stresses in agricultural products using a finite-element method," *Transactions of the ASAE*, vol. 20, no. 1, pp. 162–167, 1977.

[12] E. Dintwa, M. Van Zeebroeck, H. Ramon, and E. Tijskens, "Finite element analysis of the dynamic collision of apple fruit," *Postharvest Biology and Technology*, vol. 49, no. 2, pp. 260–276, 2008.

[13] H.-Z. Song, J. Wang, and Y.-H. Li, "Studies on vibration characteristics of a pear using finite element method," *Journal of Zhejiang University Science B*, vol. 7, no. 6, pp. 491–496, 2006.

[14] E. Dintwa, P. Jancsók, H. K. Mebatsion et al., "A finite element model for mechanical deformation of single tomato suspension cells," *Journal of Food Engineering*, vol. 103, no. 3, pp. 265–272, 2011.

[15] C. X. Wang, J. Pritchard, and C. R. Thomas, "Investigation of the mechanics of single tomato fruit cells," *Journal of Texture Studies*, vol. 37, no. 5, pp. 597–606, 2006.

[16] M. Van Zeebroeck, E. Tijskens, E. Dintwa et al., "The discrete element method (DEM) to simulate fruit impact damage during transport and handling: model building and validation of DEM to predict bruise damage of apples," *Postharvest Biology and Technology*, vol. 41, no. 1, pp. 85–91, 2006.

[17] A. O. Raji and J. F. Favier, "Model for the deformation in agricultural and food particulate materials under bulk compressive loading using discrete element method. I: theory, model development and validation," *Journal of Food Engineering*, vol. 64, pp. 359–371, 2004.

[18] J. Garjonis, R. Kacianauskas, E. Stupak, and V. Vadluga, "Investigation of contact behaviour of elastic layered spheres by FEM," *Mechanika*, vol. 3, no. 77, pp. 5–12, 2009.

[19] R. Goltsberg, I. Etsion, and G. Davidi, "The onset of plastic yielding in a coated sphere compressed by a rigid flat," *Wear*, vol. 271, no. 11-12, pp. 2968–2977, 2011.

[20] R. Mercadé-Prieto, C. R. Thomas, and Z. Zhang, "Mechanical double layer model for *Saccharomyces Cerevisiae* cell wall," *European Biophysics Journal*, vol. 42, no. 8, pp. 613–620, 2013.

[21] G. Sitkei, *Mechanics of Agricultural Materials*, Elsevier, New York, NY, USA, 1986.

[22] P. Guillermin, N. Dupont, C. Le Morvan, J.-M. Le Quéré, C. Langlais, and J. C. Mauget, "Rheological and technological properties of two cider apple cultivars," *LWT—Food Science and Technology*, vol. 39, no. 9, pp. 995–1000, 2006.

[23] A. Allende, M. Desmet, E. Vanstreels, B. E. Verlinden, and B. M. Nicolaï, "Micromechanical and geometrical properties of tomato skin related to differences in puncture injury susceptibility," *Postharvest Biology and Technology*, vol. 34, no. 2, pp. 131–141, 2004.